



Giant Radio lobes of Centaurus A studied with the Chandra



K. Balasubramaniam^{4,1}

Collaborators : Sayantan Ghosh, Łukasz Stawarz¹, Chang Hsiang-Kuang⁴, V. Kashyap² & V. Marchenko¹

¹ Astronomical observatory, Jagiellonian university-Krakow, Poland

² Harvard Smithsonian Center for Astrophysics, USA

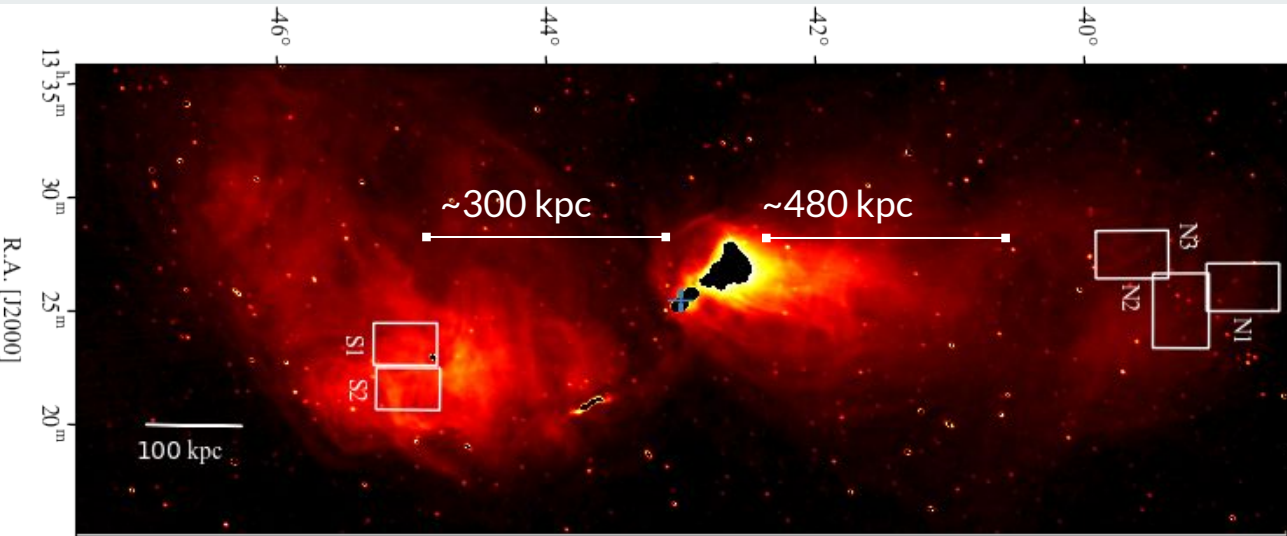
³ Space Science Division, Naval Research Laboratory, USA

⁴ Institute of Astronomy, National Tsing Hua University, Hsinchu, Taiwan



Giant Radio Lobes of Centaurus A

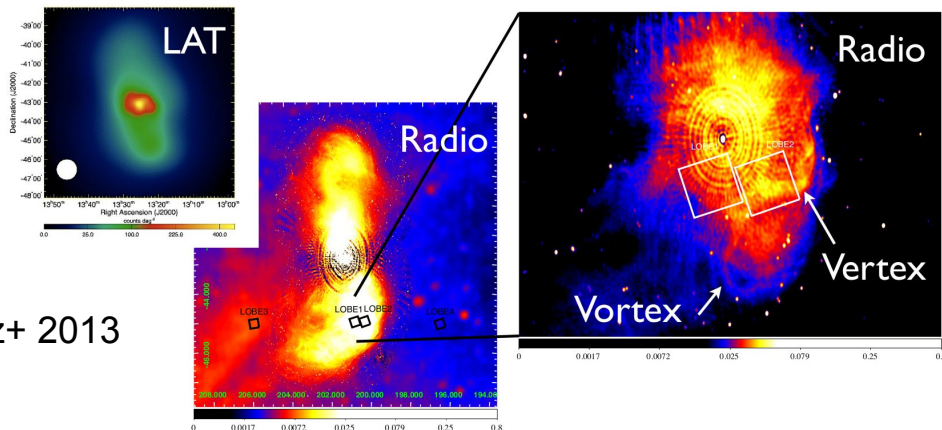
Dec: [J2000]



- Flat Λ -CDM (Planck XIII 2016): $H_0=67.8$, $\Omega_m=0.308$
- $z=0.001830$ (Spoon+2022)
- Distance = 3.8 ± 0.1 Mpc (Harris+2010)
- Scale: $1^\circ \approx 0.1409$ Mpc
- $D_A=8.068$ Mpc, $D_L=8.1$ Mpc
- Age at $z = 11.596$ Gyr

Region	Distance from center (kpc)
S1	306.042
S2	314.197
N1	575.449
N2	461.210
N3	523.541

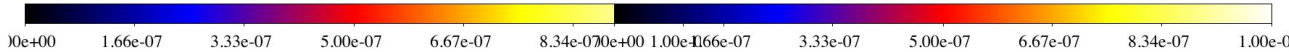
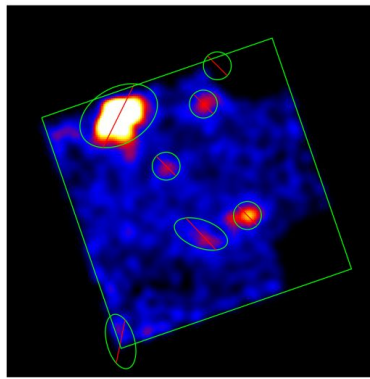
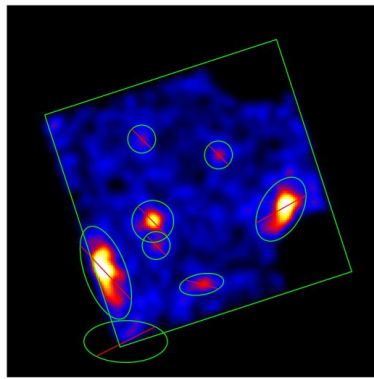
Adapted from McKinley+2022
MWA @ 185MHz



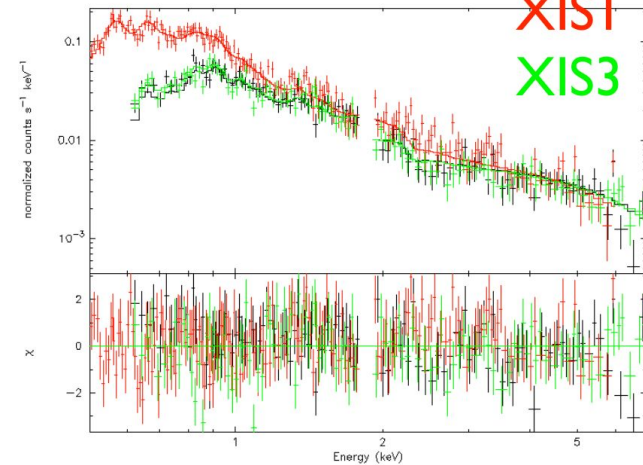
Stawarz+ 2013

Lobe spectrum

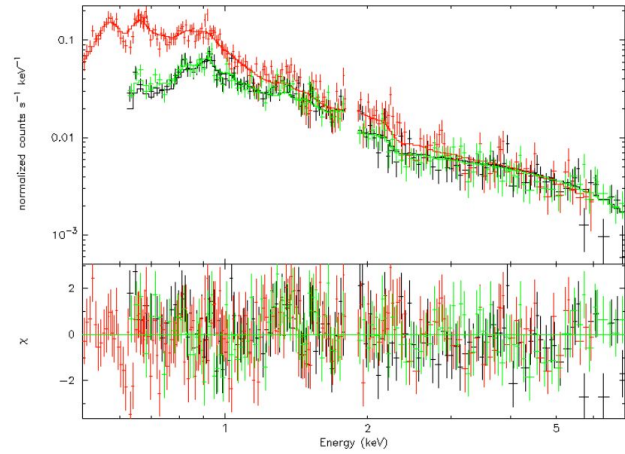
- mekal+wabs*(mekal+p(w)), which corresponds to Local hot bubble, Galactic halo, and cosmic X-ray background



Stawarz+ 2013 Lobe 1 **XIS0**
data and folded model



Lobe 2
data and folded model



- 1.8-1.9 keV were ignored due to calibration uncertainty of Si K-edge (1.84 keV)
- In the fit, 0.6-7.0 keV were utilized for XIS0 and 3, and 0.5-6.0 keV for XIS1

Modeling Results for the Diffuse Emission

Region (1)	kT_{LB} (2)	Norm_{LB} (3)	kT_{GH} (4)	Norm_{GH} (5)	Norm_{CXB} (6)	$F_{0.5-2\text{keV}}^{\text{abs}}$ (7)	$F_{2-10\text{keV}}^{\text{abs}}$ (8)	Z/Z_{\odot} (9)	Red. χ^2/dof (10)
Lobe 1 (“on”)	0.19 ± 0.01	$3.53^{+0.20}_{-0.20}$	$0.60^{+0.03}_{-0.03}$	$7.42^{+0.79}_{-0.82}$	$0.97^{+0.03}_{-0.02}$	7.88	6.32	1.0^f	1.16/441
Lobe 2 (“on”)	0.20 ± 0.01	$3.22^{+0.18}_{-0.17}$	$0.66^{+0.02}_{-0.03}$	$7.38^{+0.68}_{-0.69}$	$1.01^{+0.03}_{-0.02}$	7.67	6.59	1.0^f	1.13/512
Lobe 3 (“off”)	0.20 ± 0.01	$3.30^{+0.33}_{-0.32}$	$0.70^{+0.12}_{-0.09}$	$3.79^{+1.28}_{-1.16}$	$1.04^{+0.05}_{-0.05}$	7.19	6.73	1.0^f	1.30/131
Lobe 4 (“off”)	0.19 ± 0.01	$2.34^{+0.33}_{-0.31}$	$0.80^{+0.16}_{-0.13}$	$3.45^{+0.88}_{-0.84}$	$1.18^{+0.05}_{-0.06}$	5.87	7.63	1.0^f	0.87/123

Notes. (1) Region fitted; (2) temperature of the LB component in keV units; (3) MEKAL normalization of the LB component $\times 10^{-3}$; (4) temperature of the GH component in keV units; (5) MEKAL normalization of the GH component $\times 10^{-4}$; (6) normalization of the CXB component $\times 10^{-3}$; (7) absorbed 0.5–2 keV flux in units of 10^{-12} erg cm $^{-2}$ s $^{-1}$ /0.35 deg 2 ; (8) absorbed 2–10 keV flux in units of 10^{-12} erg cm $^{-2}$ s $^{-1}$ /0.35 deg 2 ; (9) fixed (“f”) abundance; (10) reduced χ^2 value/degree of freedom.

Excess soft emissions seems present for both two “on” pointings, around 0.8 keV

Region (1)	Z_{GH}/Z_{\odot} (2)	kT_{GH} (3)	Norm_{GH} (4)	Z_{ext}/Z_{\odot} (5)	kT_{ext} (6)	Norm_{ext} (7)	Γ_{CXB} (8)	Norm_{CXB} (9)
Lobe 1 (“on”)	1.0^f	$0.16^{+0.01}_{-0.02}$	$7.34^{+3.48}_{-1.52}$	0.3^f	0.59 ± 0.02	3.60 ± 0.17	1.41^f	1.04 ± 0.02
Lobe 2 (“on”)	”	”	”	”	0.73 ± 0.02	3.15 ± 0.15	”	”
Lobe 3 (“off”)	”	”	”	”	0.71 ± 0.11	1.43 ± 0.27	”	$1.30^{+0.04}_{-0.03}$
Lobe 4 (“off”)	”	”	”	”	1.59 ± 0.36	1.31 ± 0.30	”	”

Notes. (1) Region fitted; (2) fixed (“f”) abundance of the GH component; (3) temperature of the GH component in keV units; (4) APEC normalization of the GH component $\times 10^{-3}$; (5) fixed (“f”) abundance of the extra thermal component; (6) temperature of the extra thermal component in keV units; (7) APEC normalization of the extra thermal component $\times 10^{-3}$; (8) fixed (“f”) photon index of the CXB component; (9) normalization of the CXB component $\times 10^{-3}$.

Table 4
Modeling Results for the X-Ray Spots Detected at $>5\sigma$ Level

Source (1)	Red. χ^2 /dof (2)	Γ (3)	$F_{x, \text{abs}}$ (4)	F_x (5)	Red. χ^2 /dof (6)	kT (7)	$F_{x, \text{abs}}$ (8)	F_x (9)	Z/Z_\odot (10)	Norm (11)	Red. χ^2 /dof (12)
src 3	1.340/8	$1.32^{+0.12}_{-0.12}$	29.2	30.4	0.671/51	32.8	28.3	29.5	0.3^f	$17.1^{+3.6}_{-2.2}$	0.639/52
src 5	0.211/8	$2.00^{+0.35}_{-0.32}$	6.6	7.3	1.192/30	$4.6^{+4.7}_{-1.6}$	6.3	6.8	0.3^f	$4.77^{+0.81}_{-0.82}$	1.249/31
src 6	0.395/8	$1.89^{+0.24}_{-0.21}$	7.5	8.3	0.804/36	$4.6^{+2.6}_{-1.3}$	6.9	7.4	0.3^f	$5.24^{+0.66}_{-0.67}$	0.788/37
src 7	0.693/8	$2.52^{+0.24}_{-0.23}$	7.1	8.3	1.020/38	$2.1^{+0.7}_{-0.3}$	5.8	6.5	0.3^f	$6.55^{+0.69}_{-0.69}$	1.373/39
src 8	0.598/8	$1.68^{+0.14}_{-0.14}$	15.8	16.8	0.685/47	$7.3^{+4.3}_{-2.1}$	14.9	15.8	0.3^f	$9.57^{+0.73}_{-0.71}$	0.770/48

Notes. (1) Source ID; (2) quality of a constant fit to the source light curve (reduced χ^2 value/degree of freedom); (3) photon index in the PL model with 90% confidence level errors; (4) absorbed 0.5–10 keV flux of the source in the PL model, in units of 10^{-14} erg cm^{-2} s^{-1} ; (5) unabsorbed 0.5–10 keV flux of the source in the PL model in the same units; (6) quality of the PL fit; (7) plasma temperature for the APEC model in units of keV with 90% confidence level errors (except for src 3, for which no meaningful errors could be calculated); (8) absorbed 0.5–10 keV flux of the source in the APEC model, in units of 10^{-14} erg cm^{-2} s^{-1} ; (9) unabsorbed 0.5–10 keV flux of the source in the APEC model in the same units; (10) fixed (“ f ”) abundance in the APEC fit; (11) APEC normalization $\times 10^{-5}$; (12) quality of the APEC fit.

- Due to bad statistics, it was not possible to distinguish between thermal and non-thermal
- Fit with Thermal plasma or non-thermal PL

The FoV is filled with $kT \sim 0.5$ keV thermal gas ($P_g \sim 8 \times 10^{-14}$)

Is Thermal emission has too high pressure? $n_g kT \sim 10^{-10} R_{1.5}^{-3/2}$

Materials and Methods

Data Reduction

- Raw ACIS-I observations (Chandra proposal 14900703, cycle 14) for five regions (see Tab.1) were used for this study.
- Reduction using CIAO-4.15.1 with CALDB-4.10.4 (Fruscione+2006)
- Energy separation in Broad (0.5–7.0keV), Soft (0.5–1.2keV), Medium (1.2 – 2.0keV), and Hard (2.0 – 7.0keV) bands.
- Identification of point sources using *wavdetect* (Freeman+2002) with *sigthresh* = 1.23×10^{-8} corresponding to a false count rate of 1 per 81M pixels.
- Counts, flux, spectra, and light curve extraction in each energy band for individual sources using *srcflux* ($\Gamma=2.0$) and *%GAL* (Davis+2012) for adaptive galactic absorption) at 3σ confidence level.

Characterization :

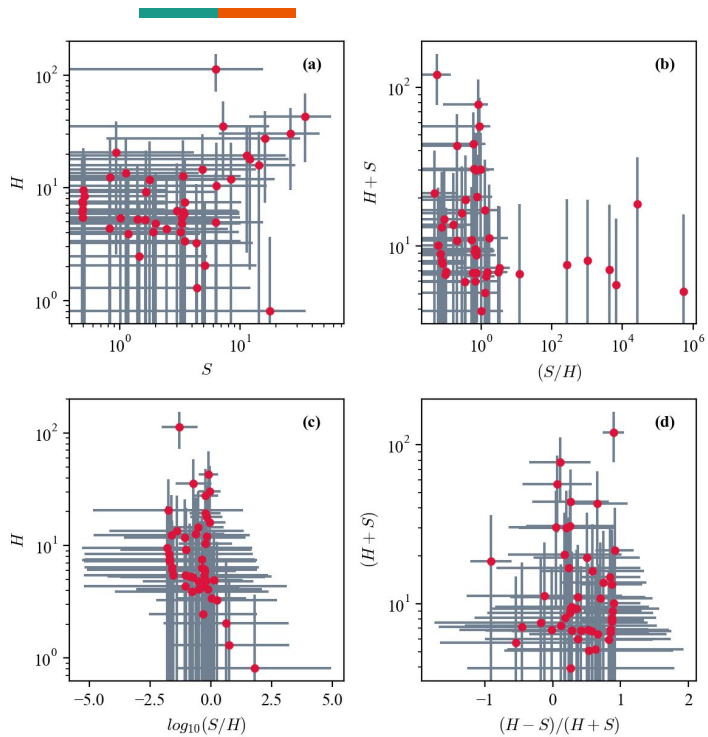
- Hardness Ratios: HR_{HS} , HR_{HM} , HR_{MS} and X-ray colors C_{HS} , C_{HM} , C_{MS} using *BEHR* (Park+2006).
- Cross matching with *GAIA DR3*, *AllWISE*, *2MASS*, and *GALEX* for spectral energy distribution fitting to be done using *CIGALE* (Yang+2022)

Region	Chandra ObsID	RA J2000	DEC J2000	Size W × H	Wavdetect	CSC v2.0.1	GAIA DR3	AllWISE
S1	15199	200.86	-45.16	0.44° × 0.47°	34	25	19	19
S2	15200	200.39	-45.14	0.44° × 0.47°	41	31	17	25
N1	15201	201.47	-38.94	0.45° × 0.54°	52	37	13	29
N2	15202	201.78	-39.76	0.46° × 0.54°	40	24	11	21
N3	15203	201.16	-39.31	0.72° × 0.42°	47	29	11	30
Totals					214	146	71	124

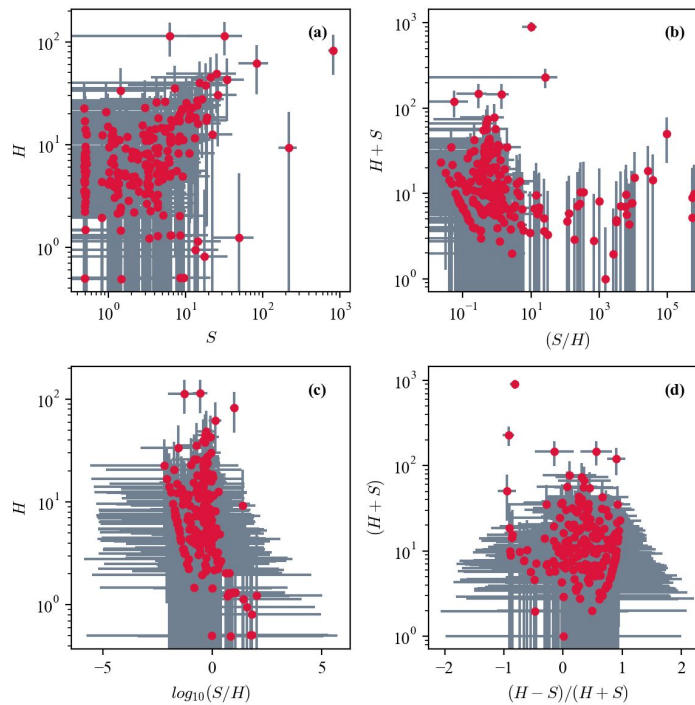
No counterparts in GALEX AIS 5+6

Hardness Ratio

15203 N3



Combined



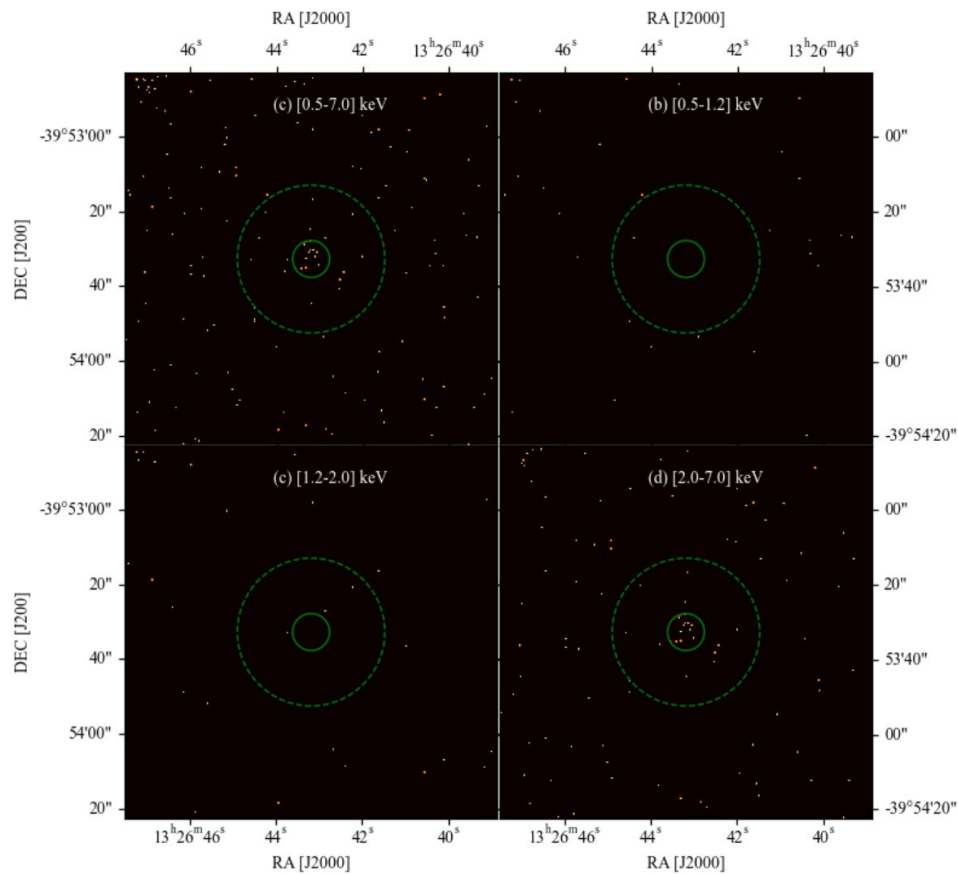
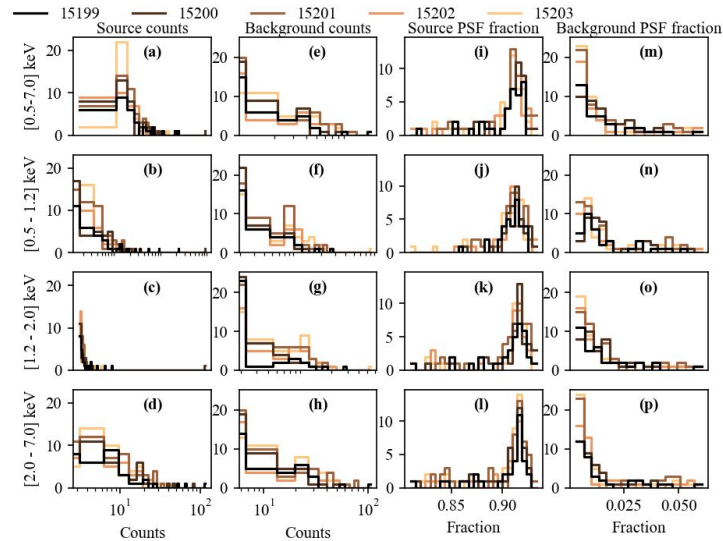


Figure 2: An example of a hard X-ray source at $13^{\text{h}}26^{\text{m}}43.19^{\text{s}}$, $-39^{\circ}53^{\text{m}}32.69^{\text{s}}$ identified in N2.

- A wide variation of low count and band-specific sources. See Fig.2 for a hard X-Ray source.
- The counts statistics for the five regions in the Broad, Soft, Medium and Hard bands $3\sigma \sim 99.73\%$ confidence levels are shown in Fig.3. The GRL are a low X-ray count region, with a few notable exceptions appearing in the soft and hard bands.
- The hardness ratios for the region S1 are shown in Fig. 4. The significant population of purely hard sources contribute to the top left and bottom right of the panels (a) and (b).

Counts statistics from srcflux



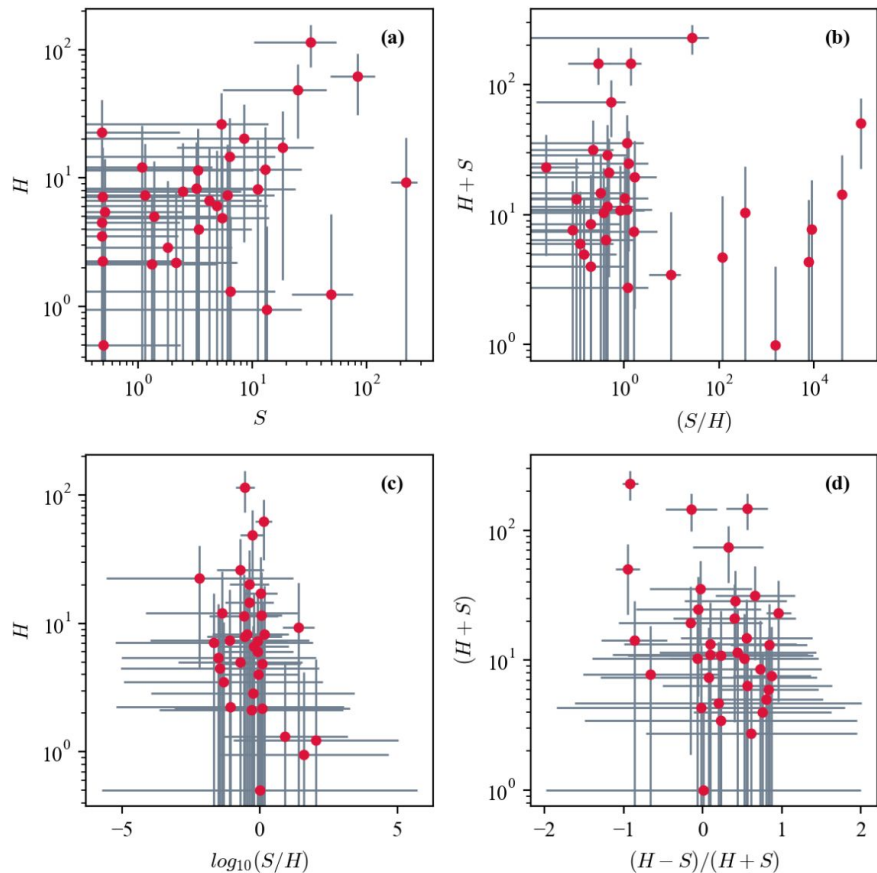


Figure 4: Hardness ratios and color diagrams for the sources in the S1 region at 3σ confidence level.

SUMMARY

1. We present a consolidated **pipeline** to identify and *characterise point like sources* in arbitrarily large-scale studies of Chandra observations.
2. We find the GRL to be a *low X-ray count region*, with slightly higher emissions in the sparse **northern lobes** for **soft X-rays**, with the **southern lobe** contributing more to the **hard X-rays**.
3. *Higher photon counts above 3 keV* could possibly be influenced by **ionisation or non-thermal processes**.
(L. Stawarz +13)
4. Possible identification of previously undiscovered sources, characterisation in progress.

Currently, looking for positions

Research Experience

- Aug 2022 – **Postdoctoral Fellow**, *National Tsing Hua University, Taiwan*, with the supervision of Dr. Hsiang-Kuang Chang.
July 2023
- Dec 2021 – **Associate**, *Astronomical Observatory of the Jagiellonian University, Kraków Poland*.
- Oct 2016 – **Ph.D. in Exact and Natural Sciences of Astronomy**, *Astronomical Observatory of the Jagiellonian University, Kraków Poland*.
Nov 2021
 - “**Fluorescent Iron Lines in Various Types of Radio-Loud Active Galactic Nuclei**” under the supervision of Dr hab. Łukasz Stawarz and co-advisor Dr. Volodymyr Marchenko.
- Apr 2015 – , **M.Sc. Project**, Indian Institute of Astrophysics, India.
Jun 2016 under the supervision of Dr F.K. Sutaria and Dr Subinoy Das, Indian Institute of Astrophysics, India “**Unidentified Emission line in Stacked X-ray spectra of Dwarf galaxies , looking for Dark matter candidates**”.
- Jan 2014 – , **Visiting Intern Student**, Indian Institute of Astrophysics, India.
Sept 2014 “**Dynamic Loading Assembly for Performance Testing of Segmented Mirror Telescope Actuator**” Worked under the supervision of Dr Padmakar Singh Parihar .

Orcid : <https://orcid.org/0000-0003-0095-9302>

1. K. Balasubramaniam et al in prep.(2023) : **Giant Radio Lobes of Centaurus A, Studied with the Chandra X-ray Observatory**
2. K. Balasubramaniam et al in prep.(2023) : **Black Hole Spins in AGNs: A Systematic Perspective**

